Chapter 1

Introduction

Atomic nuclei are endowed with a large variety of structures and a major classification of these is in terms of single particle, collective (representing co-operative motion among the nucleons) and statistical (representing a type of random or chaotic motion) features. These three structures are distinctly seen in some selective nuclei in selective energy domains; for example the low energy spectrum of (^{40}K, ^{42}Ca), levels upto about 2.5 MeV excitation in ^{168}Er and resonances at neutron separation energy in ^{238}U respectively, clearly show the above three features. These three structures led to the development of the nuclear shell model by Mayer and Jensen [Ma-65], geometric models by Bohr and Mottelson [Bo-69, Bo-75] and statistical mechanical methods / random matrix models by Bethe and Wigner [Be-36, Wi-55].

Recognizing that the statistical features extend throughout the spectrum of a complex nucleus [Br-81], the scope of statistical approach to nuclear structure was enlarged by French [Fr-67, Fr-69a, Ch-71, Fr-72, Mo-75, Dr-77a, Dr-77b, Fr-79], by combining shell model ideas with Bethe and Wigner's treatment of statistical properties of nuclei, by introducing and developing the subject of

statistical nuclear spectroscopy. Before proceeding further it should be stressed that statistical spectroscopy provides a path for understanding the deeper connections between symmetries, statistical behavior and quantum chaos on one hand and information propagation on the other in complex nuclei (in general in complex many body systems); see Fig. 1.1. Statistical spectroscopy divides into two parts, spectral average being one part and fluctuation (around the averages) being the other with little communication between the two. The origin and nature of the separation is understood analytically by using ensemble of hamiltonian matrices [Mo-75] and two good numerical examples are also available [Br-81, La-90]. The separation gives a permit to deal with averages and fluctuations separately and by using different methods. The model for energy level and strength fluctuations is the so called GOE (Gaussian orthogonal ensemble of random matrices) model. It is well known that GOE describes fluctuations in slow neutron resonance domain to a very high degree of precision [Ha-82a] and also GOE is closely connected with 'quantum chaos' [Bo-84, Bo-88]. The Dyson Mehta [Dy-63] spectral rigidity ensures that spectral fluctuations are small and they essentially carry no information except for symmetries (Ref. [Fr-88a, Fr-88b] gives a good example where a bound on the size of time reversal non-invariant (TRNI) part of nucleon-nucleon interaction is derived from slow neutron resonance data). Hence fluctuations can be ignored for most purposes and spectral averages carry most of the significant physical information about observables [1]. The theory that allows one to derive

[1] All spectroscopic observables, broadly speaking, belong to one (or products) of the three basic quantities: (1) state density $I(E)$ which counts the number of states in the interval E and $E + \Delta E$, or its normalized version $\rho(E)$, (2) expectation values $\langle K \rangle^E$ – diagonal matrix elements of an operator K in the hamiltonian (H) diagonal basis or expectation value densities $I_K(E) = \langle K \rangle^E I(E)$, and (3) strengths $|\langle E'|\mathcal{O}|E\rangle|^2$ – squares of matrix elements connecting two H-eigenstates or strength densities $\mathbf{I}_\mathcal{O}(E, E') = I(E')|\langle E'|\mathcal{O}|E\rangle|^2 I(E)$. Energies are also observables and they are tacitly included in (1) above.

Figure 1.1

Typical spectrum of a heavy nucleus. Figure is taken from [Fr-89c]. As French and Kota state [Fr-89c]: "If we start at the ground state and go up in the spectrum of such a nucleus we can identify in order the following domains: (D1) the shell model domain (0-2 MeV); (D2) no man's land (2-6 MeV); (D3) the fluctuation window (6 - 6.002 MeV); (D4) the true continuum ($>$ 6.002 MeV), where typical values are given for the domain boundary energies which of course vary somewhat from nucleus to nucleus. The two domains D1, D3 where spectra can be studied in exquisite detail, contain no more than a few hundred states at best and are separated by D2 which contains many millions of states about which because of experimental limitation, almost nothing is known. ..... Up to now there have been for example no serious attempts to cross the no-man's land and calculate from the D1 spectrum and the general features of the interaction, the absolute state or level density in the resonance region D3, (the only part of the complete spectrum where unambiguously-defined smoothed densities have been measured with some precision)..... We justify our description of D1 as the "shell-model domain" by the argument that the shell model supplies the foundation for most microscopic models. D1 is of course extraordinarily rich in experimental data, and in theoretical concepts and models which involve, among other things, a wide range of symmetries with their more-or-less-well conserved quantum numbers. Some of the D1 data, yrast states and giant resonances for example, do extend to higher domains, but since these extensions involve only a small fraction of the states in the upper domains, this does not negate our classification. In D2 a transition occurs from a spectrum (of D1) which is profitably studied in detail, level by level, to one (of D3) in which the only sensible treatment would appear to be statistical one. (..... one must distinguish between the use of *statistical methods* (as in our use of central limit theorems for the state density generated by a given Hamiltonian) and *statistical assumptions* (as with fluctuations where we assume *a priori*, and justfy by the results that averaging over a Hamiltonian

ensemble is an appropriate procedure)). One might take for granted that we proceed to such a treatment of D3 because the D3 complexities make it impossible to do better. After all only a part of the spectrum is available (often only the $1/2^+$ levels; see below), the shell model spaces are enormous (dimensionality $\sim 10^{15} - 10^{30}$; the present diagonalization limit is $\sim 10^4$), and not enough could be known about the Hamiltonian, or deduced from the data, to support such a study. These practical reasons however are essentially irrelevant. The real point is that, just as the introduction of temperature and entropy concepts into mechanics give us a completely new view of things, so also with D3 spectrum which gives an extraordinary "window" through which we can study important aspects of a quantum-chaotic system; indeed it gives by far the best experimental data on quantum chaos available now for any real system. ..... The latter effect weakens, and the resonances broaden, as the neutron energy increases and the resultant overlapping of levels marks the beginning of the true continuum D4. In the lower part of D4 the effects due to underlying resonances can still be observed as Ericson cross-section fluctuations. ..... our study of the D1 - D3 relationship splits into two parts. The first, the 1-point problem, is the extension of the *detailed* D1 spectrum into the *smoothed* level density of D3 and then to other domains both above and below D3. The second part is the study, and comparison with data of the spectral fluctuations ....."

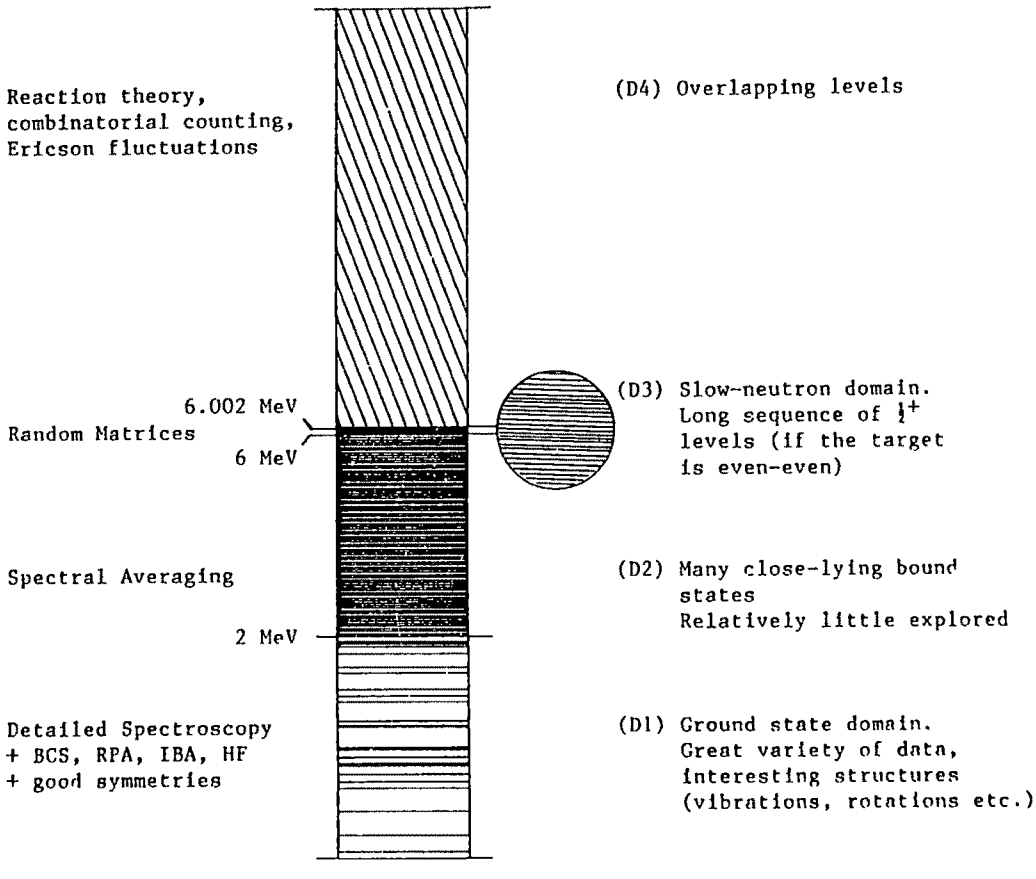

Typical Spectrum of a Heavy Nucleus

and apply the smoothed (with respect to energy) forms of spectroscopic observables is called spectral averaging theory (SAT) and the resulting method for nuclear spectroscopy studies is often called spectral distribution methods (SDM). The subject matter of this thesis is SAT/SDM.

The fundamental result based on which SAT is developed is that there are central limit theorems (CLT's) operating in nuclear shell model spaces. We begin with state densities. For a non-interacting particle (NIP) system (i.e. ignoring interaction) energies are additive and then the m - particle eigenvalue density (state density $I(E)$) is an m - fold convolution of one-particle density which in general tends to a Gaussian ($\mathcal{G}$), due to CLT, very rapidly as m increases. The remarkable result is that even with interactions, though the energies are no longer additive, state densities take Gaussian form. This feature is demonstrated in an example in Fig. 1.2. The origin of CLT for interacting particle (IP) systems lies in an ensemble representation of the IP hamiltonian (H). As studied by Mon and French [Mo-75], the appropriate ensemble is the so called embedded Gaussian orthogonal ensemble generated (in m - particle spaces) by k - body interactions or EGOE(k) [2]; for nuclear case $k = 2$. With EGOE(k), in the dilute limit ($m \rightarrow \infty$, $N \rightarrow \infty$, $k << m$, $m/N \rightarrow 0$) one sees immediately that the lower order cumulants tend to zero; for example the excess parameter $\gamma_2 \sim -k^2/m \rightarrow 0$ as $m \rightarrow \infty$ and $k << m$. Thus in the CLT limit state densities take a Gaussian form and in practice one can add the skewness and excess corrections (Edgeworth corrections described in Chapter 2) to the Gaussian. Inverting the distribution function

[2] In general in nuclear shell model, EGOE(k) for m ($m > k$) particle systems is generated by defining the H to be GOE in k - particle spaces and then propagating it to m - particle spaces by using the geometry of the shell model spaces.

Figure 1.2

Density of states $I(E)$ (in MeV^{-1}) vs energy E. The histogram is for the shell model results where the calculations are made in $(ds)^{6,J=2\,T=0}$ space with (KUO+^{17}O) interaction [Ku-67]. The smooth curve is the Gaussian approximation. The dimensionality (d) of the space, centroid E_c, variance σ, skewness γ_1 and excess γ_2 are also shown in the figure. Figure is taken from [Ko-89].

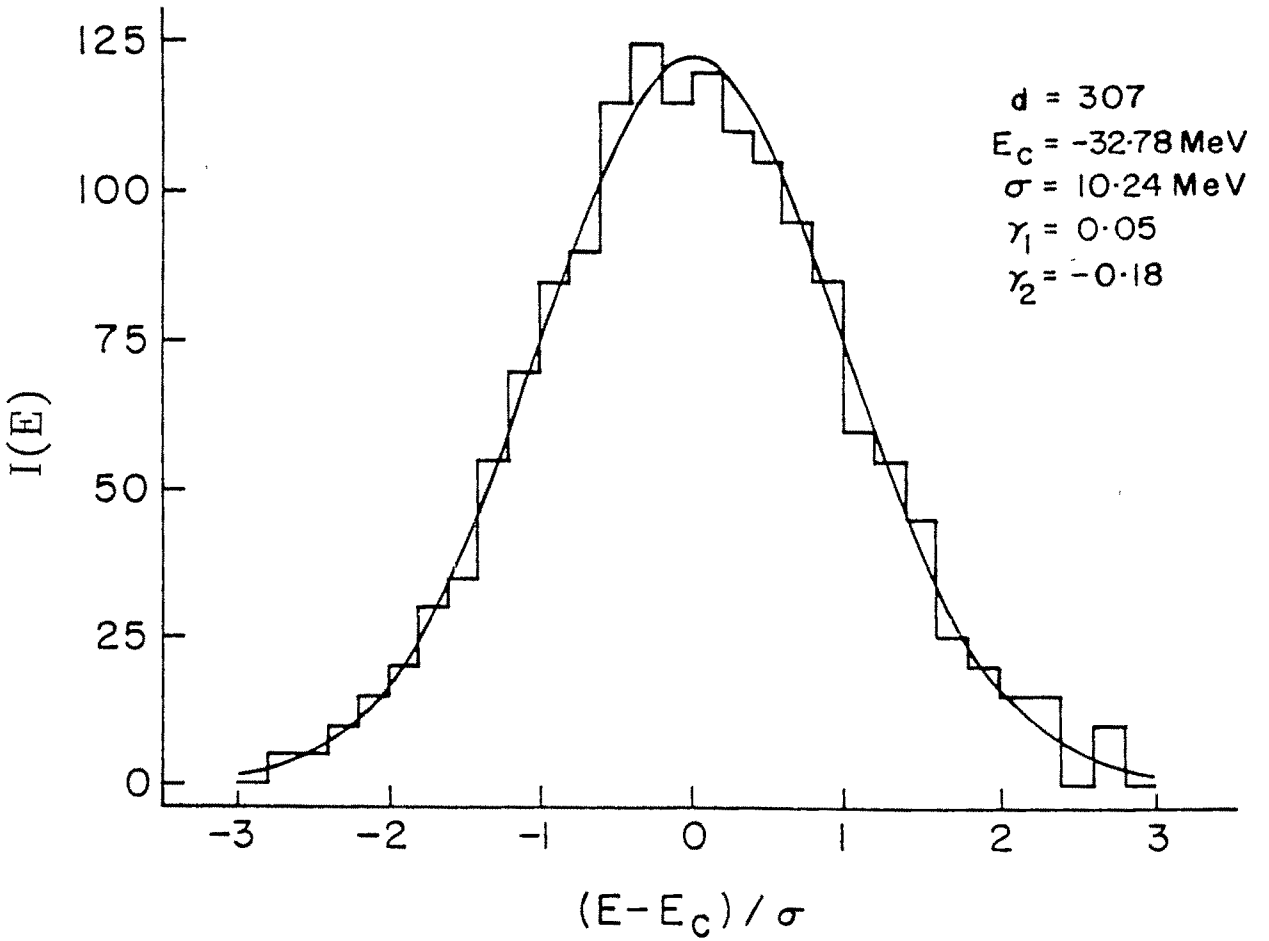
125
100
75
50
25
0
I(E)
-3
-2
-1
0
1
2
3
(E-E_C) / σ
d = 307
E_C = -32·78 MeV
σ = 10·24 MeV
γ_1 = 0·05
γ_2 = -0·18

$F(E)$ ($F(E) = \int_{-\infty}^{E} I(E)dE$) gives the smoothed spectrum [Ra-71] with deviations from the corresponding exact ones by $\sim 2\ MeV$ for ds-shell nuclei and even less for heavy nuclei. Using the polynomials defined by the state density or otherwise, lead to CLT forms for expectation values of operators and the corresponding expectation value densities. For operators K for which $H + \alpha K$ (α is a small parameter) has a Gaussian density, then by CLT one has the remarkable result that expectation values ($(K)^E$) are linear in energy with the slope given by the correlation coefficient [3] between the operators K and H. An expression for $(K)^E$ in terms of orthogonal polynomials defined by the state densities gives this result when truncated at the first two terms, with the remaining terms giving corrections to the CLT result [Dr-77a]. A good example for the linear behavior of expectation values comes from occupancies as shown in Fig. 1.3a. In general for positive definite operators (K is $\mathcal{O}^\dagger\mathcal{O}$ type; $\mathcal{O}$ is a transition operator) the expectation value density ($I_K(E)$) in the CLT limit takes a Gaussian form [Fr-89b, Ko-89] and thus the expectation values can be written as a ratio of two Gaussians; Figs 1.3b, 1.3c give examples for these CLT results. There are in general many other forms or expansions one can derive for expectation values and they will be interrelated as they all are-derivable from the traces $\langle H^p \rangle$ and $\langle KH^p \rangle$. In addition to state and expectation value densities, transition strength densities ($\mathbf{I}_\mathcal{O}(E, E')$) also take CLT forms. In general, strength densities take bivariate Gaussian ($BIV - \mathcal{G}$) form

[3] The CLT defines a geometry [Fr-72] with norm $|K|_m$ of an operator K in m - particle spaces defined by $|K|_m = \{\langle (K - \langle K \rangle^m)^\dagger (K - \langle K \rangle^m) \rangle^m\}^{1/2}$ where the m - particle average $\langle X \rangle^m$ of an operator X is $\langle X \rangle^m = \sum_{\alpha \in m} \langle m\alpha | X | m\alpha \rangle / d(m)$; $d(m)$ is the dimensionality of m - particle space and the m - particle trace $\langle\langle X \rangle\rangle^m = d(m) \langle X \rangle^m$. The norm defined here has all the properties of an Euclidean norm. With this geometry, correlation coefficient $\zeta_{K_1 - K_2}$ between two operators K_1 and K_2 is $\zeta_{K_1 - K_2}(m) = \langle (K_1 - \langle K_1 \rangle^m)^\dagger (K_2 - \langle K_2 \rangle^m) \rangle^m / (|K_1|_m |K_2|_m)$.

Figure 1.3

Comparison of shell model results with the CLT results (with or without corrections) for expectation values and expectation value densities. (a) $d_{5/2}$ and $d_{3/2}$ orbit occupancies vs energy. The calculations are in $(ds)^{5,T=1/2}$ space and the plots are for $J = 9/2$. The wavy line represents the shell model results, - - - - line is for the CLT result (linear form derived from the polynomial expansion) and • – • – •– is by including the higher order terms in the polynomial expansion. Although the CLT (with and without corrections) results shown in the figure are obtained using the polynomial expansion, essentially similar results are also obtained by using the CLT results (Gaussian or Gaussian with Edgeworth correction) for the occupancy densities. Figure is taken from [Ko-85]. (b) $I_K(E)$ vs E and $\langle K \rangle^E$ vs E for Gamow - Teller sum-rule operator K. The energy E is in MeV. The spectroscopic space used is $(ds)^5$ and the results are for the transition (J,T) = (3/2, 1/2) to (5/2, 3/2). The dimensionality (d) of the (3/2, 1/2) space is 188. The shell model $I_K(E)$ density is shown in bins of width 2 MeV and the continuous curve is its Gaussian (CLT) representation. Similarly $\star$'s are shell model results for $\langle K \rangle^E$ and the dashed curve is its CLT approximation (ratio of the expectation value and state density Gaussians). Figure is taken from [Ko-89]. (c) Spin-cutoff density $I_{J_Z^2}(E)$ and spin-cutoff factor $\langle J_Z^2 \rangle^E$ vs E. The histogram and the boxes are shell model results and the continuous curves are the CLT results including Edgeworth corrections to the densities (the state and spin-cutoff densities are Gaussians in the CLT limit). The histogram (exact shell model) for the spin-cutoff density is constructed by averaging over a bin size of $0.2\sigma \sim 1.5\ MeV$, σ is the spectrum width. Similarly the boxes for the spin-cutoff factors are constructed by averaging over a bin size of $0.3\sigma \sim 2.3\ MeV$. All the calculations are carried out using KUO + ^{17}O interaction [Ku-67]. One sees from the figures that the CLT results (with corrections) are in excellent confirmity with the shell model results. Figure is taken from [Fr-89b].

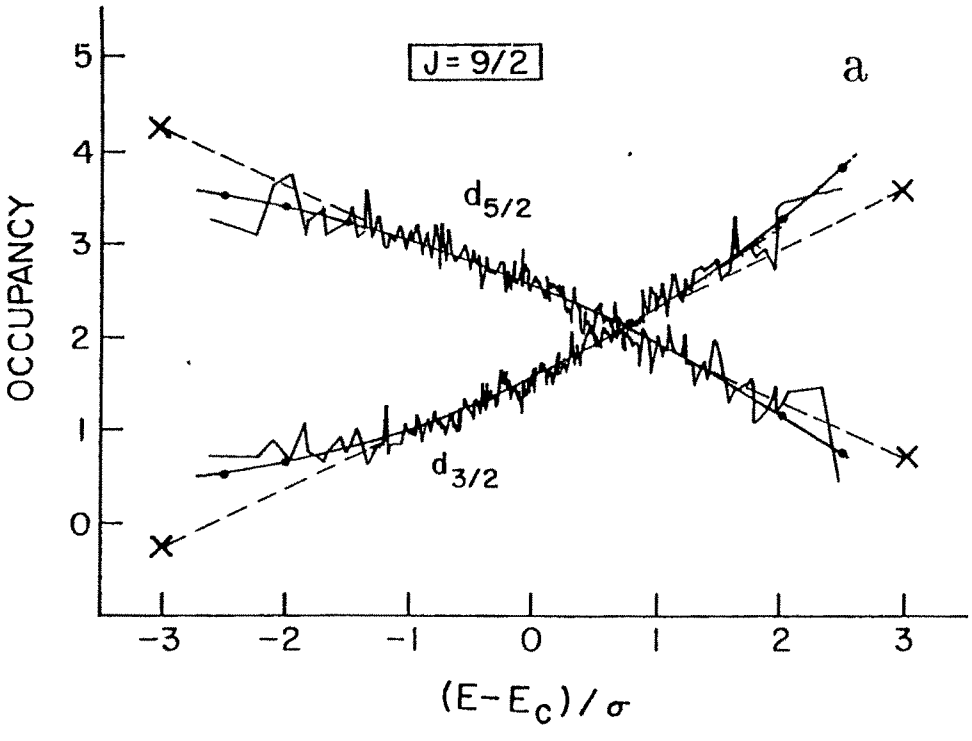
J = 9/2
a
OCCUPANCY
$d_{5/2}$
$d_{3/2}$
$(E-E_c)/\sigma$

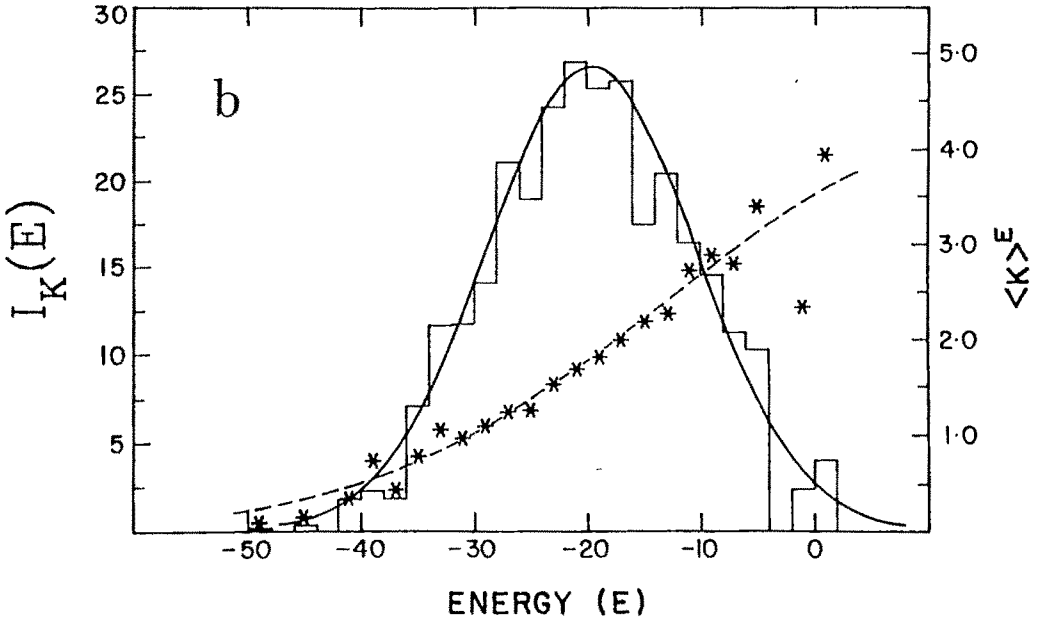
b
$I_K(E)$
$\langle K \rangle^E$
ENERGY (E)

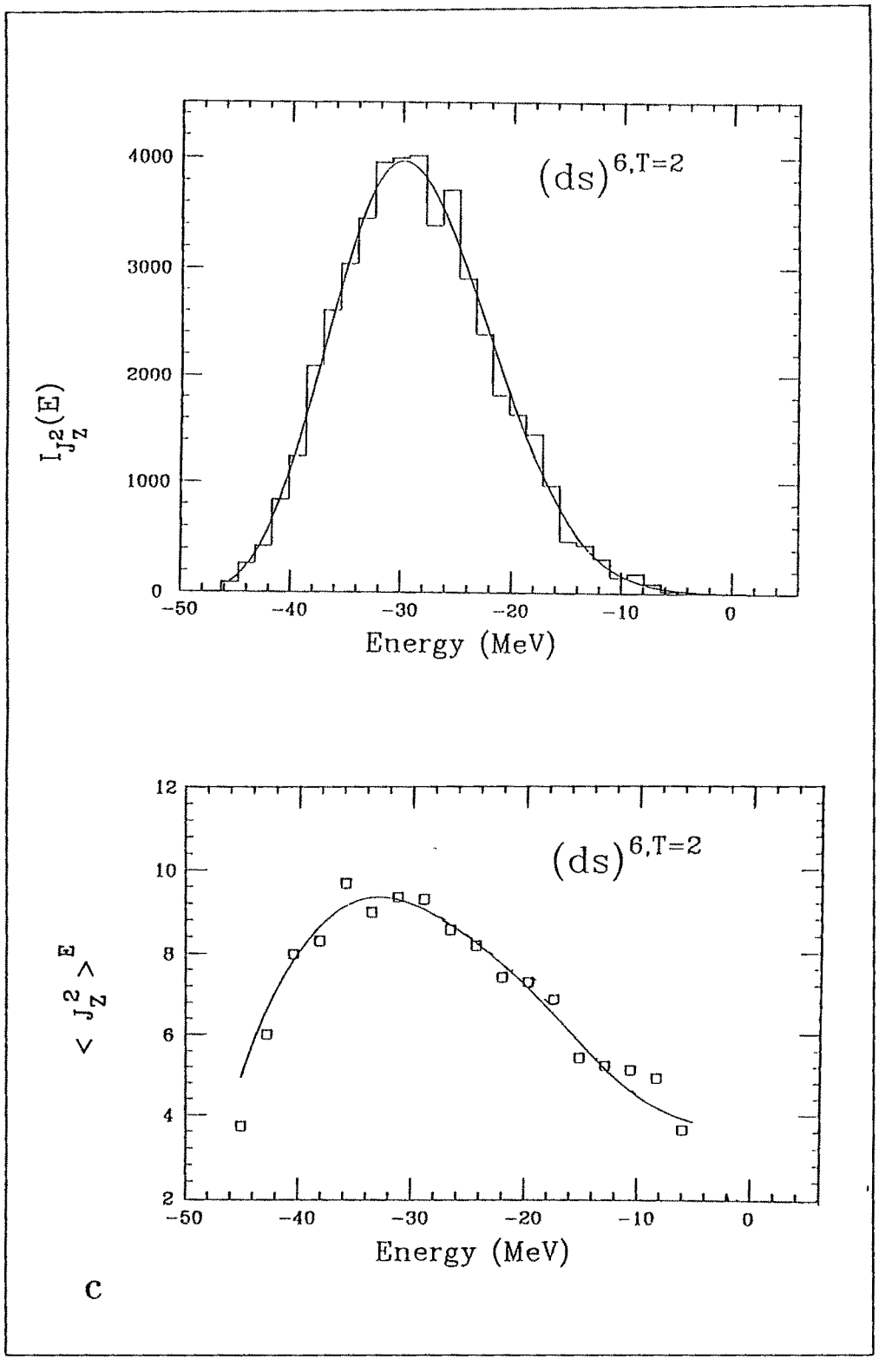
(ds)^6,T=2
$I_{J_z^2}(E)$
Energy (MeV)
(ds)^6,T=2
$<J_z^2>^E$
Energy (MeV)
C

and its origin can be understood by using ensemble (EGOE) representation for both the hamiltonian and the transition operators [Fr-88b]. This leads to the important results that the strength sum (originating from an energy E) will be a ratio of two Gaussians, the strength centroids will be linear in energy with slope given by the bivariate correlation coefficient and the strength width a constant. Fig. 1.4 gives a shell model example for these results. In addition, the CLT result for strength densities provides an understanding of the CLT result for $I_K(E)$.

The CLT results described above are in general valid only in strongly interacting shell model subspaces, i.e. essentially in $0\hbar\omega$ spaces (for example: $(ds)^8$ for ^{24}Mg and $(fp)^{16}$ for ^{56}Fe). It should be stressed that the CLT forms involve traces of products of lower order powers of operators (e.g. $I_{\mathcal{G}}(E)$ is defined in terms of $\langle H\rangle$, $\langle H^2\rangle$; $I_{K;\mathcal{G}}(E)$ by $\langle KH\rangle$, $\langle KH^2\rangle$; $\mathbf{I}_{\mathcal{O};BIV-\mathcal{G}}(E,E')$ by $\langle \mathcal{O}^\dagger H^P \mathcal{O} H^Q\rangle$ with $P+Q \leq 2$ etc.). The shell model $(0\hbar\omega)$ spaces can be partitioned into subspaces and then the state and expectation value densities decompose similarly, though there are some complications with strength densities, and the CLT results extend to the partitioned subspaces. The partitioning, on one hand takes into account the departures from CLT (smooth) forms and on the other hand brings in more information and fine structures. Much of this works in practice as the trace information propagates i.e. many particle traces can be expressed in terms of the few particle input traces, when the partitioning is done using group symmetries that can be realized in shell model spaces; for example using spherical configuration group which is a direct sum group of unitary groups, Wigner supermultiplet $SU(4)$ group etc. With this, SAT provides a formalism for addressing wide variety of nuclear structures problems. Some of the studies that are carried out in literature

Figure 1.4

Strength sum, strength centroid and strength width vs energy. The dashed curves correspond to the bivariate Gaussian (CLT) approximation for the strength density, the solid curve by including the bivariate Edgeworth corrections (given by (2.21) in Chapter 2 ahead) and the wavy curve corresponds to exact shell model results. The hamiltonian is KUO + ^{17}O interaction [Ku-67], the transition operator is the unitary two-body part ($\nu = 2$ part defined ahead in Chapter 2) of H and the space is the 307 dimensional $(ds)^{6,J=2\,T=0}$. Figure is taken from [Fr-88b].

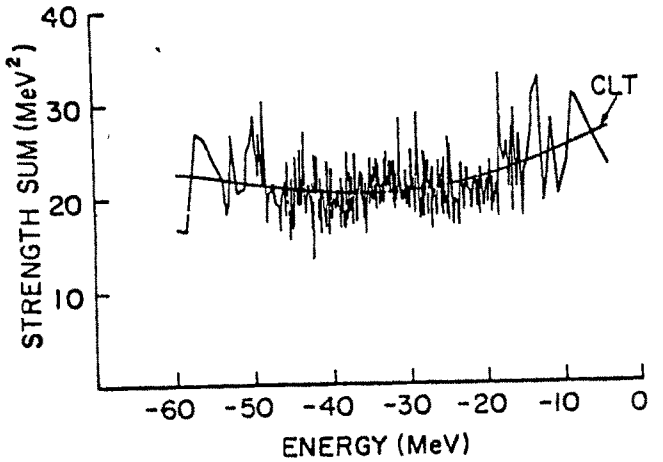
STRENGTH SUM (MeV²)
40
30
20
10
CLT
-60 -50 -40 -30 -20 -10 0
ENERGY (MeV)

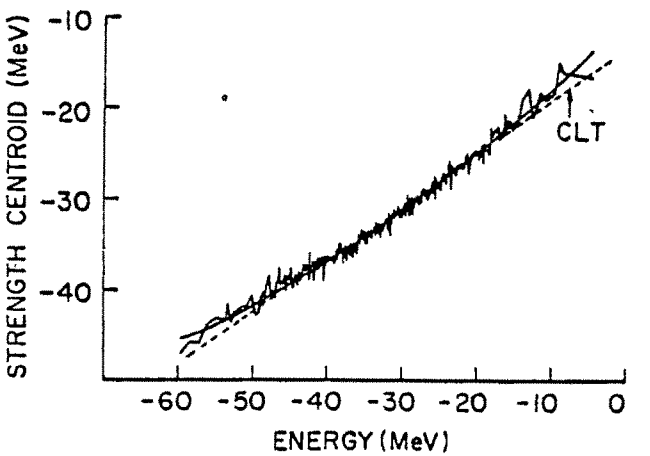
STRENGTH CENTROID (MeV)
-10
-20
-30
-40
CLT
-60 -50 -40 -30 -20 -10 0
ENERGY (MeV)

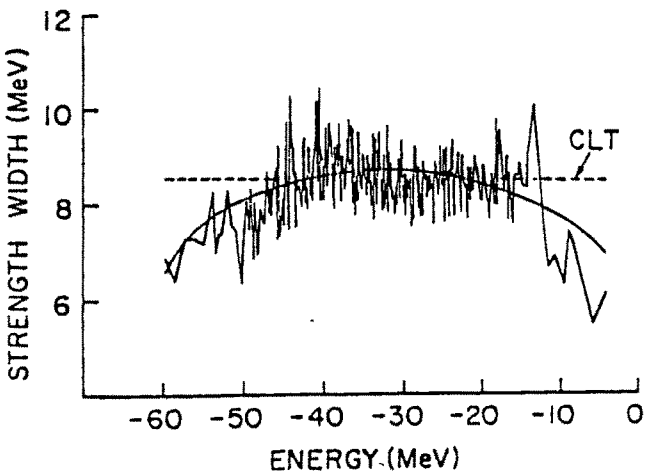
STRENGTH WIDTH (MeV)
12
10
8
6
CLT
-60 -50 -40 -30 -20 -10 0
ENERGY (MeV)

include: (i) binding energies of ds and fp-shell nuclei [Ch-71, Pa-78, Wo-86, Sa-87a]; (ii) spherical orbit occupancies for ds and fp-shell nuclei [Ch-71, Po-76, Ko-79a, Ko-82, Sa-87b]; (iii) Electromagnetic (EM) sumrules [Dr-75, Dr-77b, Ha-79, Ha-82a, Ha-82b] which include the Kurath sum rule, deriving bounds on EM summed strengths etc.; (iv) comparison and analysis of operators using the geometry (norms and correlation coefficients) defined by CLT [Ch-71, Po-77, Ko-79b, Ch-80]; (v) investigating goodness of symmetries using partial densities and their moments defined over subspaces generated by the group symmetries, good examples are the studies involving Wigner $SU(4)$, Elliot $SU(3)$ and pairing $Sp(N)$ groups [Fr-71b, Qu-74, Qu-75, Pa-78, Ch-80]; (vi) β-decay sum rule strengths and strength distributions [Ka-81, Sa-88; see also Chapter 6 ahead]; (vii) predicting collectivities [Dr-77a, Dr-77b]. As an example of the application of SAT, the analysis of $s_{1/2}$ orbit occupancies of ds-shell nuclei is shown in Fig. 1.5. The large number of studies that are carried out in $0\hbar\omega$ spaces, essentially upto 1980, are well documented [Fr-67, Fr-69a, Fr-72, Pa-78, Fr-79, Da-80, Fr-82, Fr-83a, Wo-86, Ko-89].

Recent progress in statistical spectroscopy is in deriving and applying the smoothed forms in indefinitely large shell model spaces with *interactions* by using unitary group decompositions (of hamiltonians and the spectroscopic spaces), CLT's locally, and convolutions [4] [Fr-83b, Fr-88b, Fr-89a, Fr-89b, Fr-94]. In the resulting spectral averaging theory in large shell model spaces (SAT-LSS), it is seen that the essential role of interactions is to produce local spreadings of the non-interacting particle (NIP) densities and the spreadings

[4] Convolution of two functions A and B is denoted as $A \otimes B[x] = \int_{-\infty}^{+\infty} A(y)B(x-y)dy$.

Figure 1.5

$s_{1/2}$ - ground state occupancies in SAT calculated using UNIV-SD [Wi-84], PW [Pr-72], RIP [Ha-71], KLS-R [Ka-69] and K+12FP [Ha-71] interactions compared with experimental values. The results for PW, RIP, K+12FP and KLS-R interactions and the compilation of experimental data are from [Po-76]. The results of UNIV-SD interaction are from [Sa-87b]. The analysis shown in the figure clearly demonstrates that one should exclude RIP, KLS and K+12FP interactions and favor PW and UNIV-SD interactions. The shell model results for UNIV-SD interaction show that the spectral method reproduces very well the shell model results which in turn are very close to data. All the spectral averaging calculations are done using spherical orbit configuration partitioning. Figure is taken from [Sa-87b].

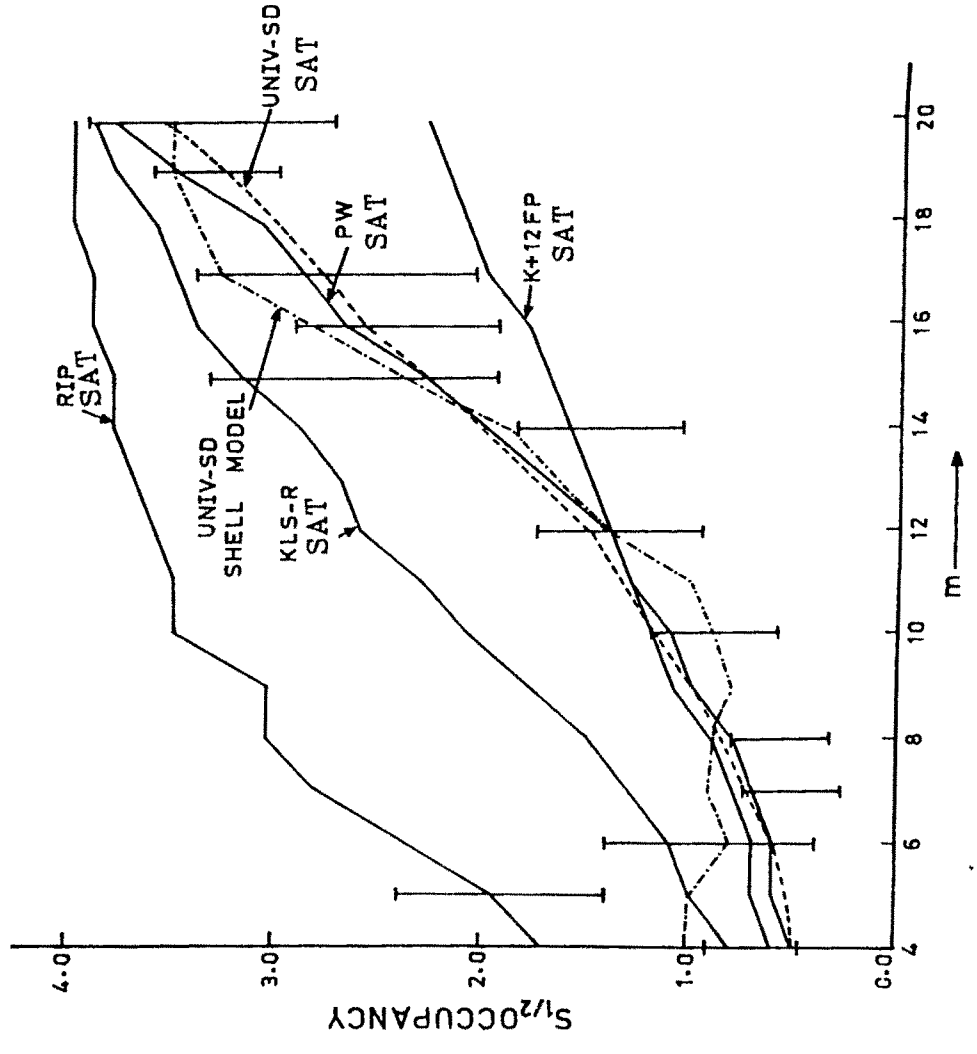
UNIV-SD SAT
PW SAT
K+12FP SAT
RIP SAT
UNIV-SD SHELL MODEL
KLS-R SAT
$S_{1/2}$ OCCUPANCY
4.0
3.0
2.0
1.0
0.0
4
6
8
10
12
14
16
18
20
m

are in general Gaussian in nature. With SAT-LSS one can calculate level densities, orbit occupancies, spin-cutoff factors [5] and other statistical observables where one needs to go beyond $0\hbar\omega$ spaces. *The aim of the present thesis is to study (and test) some aspects of this extended theory (SAT-LSS) for state, expectation value and strength densities in large spaces and apply them to calculate nuclear level densities and β-decay rates.* We will now give a preview.

Mathematical preliminaries regarding the properties of univariate and bivariate distributions, unitary group decompositions of operators, partitioning and trace propagation formulas (for cases that are of relevance for the thesis) are given in Chapter 2 along with the mathematical definitions of state, expectation value and strength densities and the corresponding CLT results (valid in $0\hbar\omega$ spaces). The results given in Chapter 2 are used throughout the thesis. Besides giving a brief overview of the convolution form for state, spin-cutoff and occupancy densities in SAT-LSS, results of systematic studies of two important aspects of SAT-LSS are given in Chapter 3 – these studies are: (a) a part of the interaction that produces non-NIP like shifts of the single particle energies, that is neglected in the theory, is demonstrated (using norms of operators) to be indeed small all across the periodic table by considering a wide variety of effective interactions; (b) moment methods for constructing locally smoothed forms for NIP state, spin-cutoff and occupancy densities are tested in a large space example including 16 spherical orbits and considering

[5] Level densities $I_\iota(E)$ count the number of levels per MeV at the given energy E; this definition can be extended for fixed angular momentum (J) and/or parity level densities (see Chapter 4 and Appendix C ahead). Spin-cutoff factors $\sigma_J^2(E)$ are nothing but the expectation values of J_Z^2 (Z - component of angular momentum J operator) operator; $\sigma_J^2(E) = \langle J_Z^2 \rangle^E$ and this definition can be extended for fixed parity spin-cutoff factors (see Appendix C ahead). Spin-cutoff factors decompose state densities into observable level densities. Finally orbit occupancies are defined by the expectation values $\langle n_\alpha \rangle^E$ where n_α is the number operator for the orbit α.

a realistic proton - neutron system. Using the convolution forms for state and spin-cutoff densities, first systematic analysis of level densities is carried out for eight fp-shell nuclei (meaningful data exist only for the eight nuclei considered) and a magnitude parameter of the effective nucleon-nucleon interaction is deduced for ^{55}Mn, ^{56}Fe, ^{59}Co, ^{60}Co and ^{60}Ni isotopes by carrying out calculations in a 8-orbit shell model space and for ^{62}Ni, ^{63}Cu and ^{65}Cu isotopes in a 10-orbit shell model space. The calculations include upto $2\hbar\omega$ excitations. The results of the fp-shell analysis are given in Chapter 4. The experimental data for all the eight fp-shell nuclei are compiled in Appendix C. Going beyond state and expectation value densities, in SAT-LSS the bivariate strength densities take a convolution form with the non-interacting particle (NIP) strength density being convoluted with a spreading bivariate Gaussian due to interactions. In order to apply this result in practice, leaving aside the question of determining the parameters of the spreading bivariate Gaussian, one needs good methods for constructing the NIP bivariate strength densities ($\mathbf{I}^h_{\mathcal{O}}$) in large shell model spaces. In Chapter 5 a formalism for constructing $\mathbf{I}^h_{\mathcal{O}}$ is developed for one-body transition operators by using spherical orbits and spherical configurations. For rapid construction and also for applying the statistical theory in large shell model spaces, $\mathbf{I}^h_{\mathcal{O}}$ is decomposed into partial densities defined by unitary orbit configurations (unitary orbit is a set of spherical orbits). Trace propagation formulas for the bivariate moments M_{rs} with $r+s \leq 2$ of the partial NIP strength densities, which will determine the Gaussian representation, are derived and the goodness of the Gaussian representation is tested in a large space numerical example using Gamow - Teller (GT) β^- transition operator. Trace propagation formulas for M_{rs} with $r+s \leq 4$ are also derived in m-particle scalar spaces which are useful for

many purposes. Construction of level densities and β-decay strength densities (in some cases even occupancy densities) have very important applications in nuclear astrophysics problems [Wo-80a]. As a first application of SAT-LSS in this important area, in Chapter 6 a method to calculate temperature dependent β-decay rates is developed by writing the expression for the rates explicitly in terms of bivariate GT strength densities for a given hamiltonian and state densities of the parent nucleus besides having the usual phase space factors. Constructing NIP GT - strength densities using the theory developed in Chapter 5, together with a simple prescription for generating the spreading bivariate Gaussians, the bivariate GT densities are constructed. Applying this theory, β-decay rates of some neutron excess fp-shell nuclei, relevant for massive presupernova stars, are calculated at presupernova matter densities, temperatures and electron fractions. In addition, the convolution form for GT densities led to a simple expression for calculating GT non-energy weighted summed strengths. Finally Chapter 7 gives concluding remarks and future outlook [6].

[6]The cut-off date for the references given in the thesis is July 1^{st}, 1994; the synopsis of this thesis was defended on July 1^{st} at the Physical Research Laboratory, Ahmedabad.